Geoderma 322 (2018) 89–100

Contents lists available at ScienceDirect

Geoderma

journal homepage: www.elsevier.com/locate/geoderma

Transport of silver nanoparticles in intact columns of calcareous soils: The role of flow conditions and soil texture

Samaneh Rahmatpour[a], Mohammad Reza Mosaddeghi[a,*], Mehran Shirvani[a], Jiří Šimůnek[b]

[a] Department of Soil Science, College of Agriculture, Isfahan University of Technology, Isfahan 84156-83111, Iran
[b] Department of Environmental Science, University of California Riverside, Riverside, CA, USA

ARTICLE INFO

Handling Editor: A.B. McBratney

Keywords:
Ag nanoparticles
Breakthrough curve
Retention profile
HYDRUS-1D
One-site kinetic attachment model
Flow condition

ABSTRACT

Growing production of manufactured nanomaterials has increased the possibility of contamination of groundwater resources and soils by nanoparticles (NPs). It is crucial to study the fate of NPs in subsurface porous media in order to evaluate and control their risks to ecosystems and human health. Hence, this study was conducted to investigate the transport and retention of polyvinylpyrrolidone (PVP) stabilized silver nanoparticles (AgNPs, a diameter of 40 nm) under saturated and unsaturated conditions in intact columns of two calcareous sandy loam (TR) and loam (ZR) soils. Furthermore, similar experiments were conducted using sand quartz as a reference medium. A pulse of the AgNP suspension with an input concentration (C_0) of 50 mg L^{-1} was injected into the columns for 3 pore volumes. The transport of bromide (Br), as a non-reactive inert tracer, was also examined. High mobility of AgNPs was observed through the sand columns due to unfavorable conditions for AgNP deposition on the quartz sand surfaces. Nearly all AgNPs introduced into the columns of both soils were retained in the soil. Percentages of AgNPs leached out of the columns were < 1% of the total injected mass in both soils. Hyperexponential retention profiles (RPs) were observed in both soils and maximum concentrations of 100–130 mg kg^{-1} were determined near the columns' inlet. However, slightly stronger retention of AgNPs and greater maximum retained concentrations on the solid phase (S_{max}) in the ZR soil compared with the TR soil may be attributed to smaller grain sizes of the ZR soil. Hydrodynamic forces adjacent to the solid surfaces near the column inlet can provide a viable explanation for the hyperexponential shape of RPs. The one-site kinetic attachment model in HYDRUS-1D, which accounted for time- and depth-dependent retention, was successfully used to analyze the retention of AgNPs. The results showed that the degree of saturation had little effect on the mobility of AgNPs through undisturbed soil columns. Our results suggested the limited transport of AgNPs in neutral/alkaline calcareous soils under both saturated and unsaturated conditions.

1. Introduction

Silver nanoparticles (AgNPs) are most commonly used for their strong antimicrobial and antiviral properties in medicine, dentistry, cosmetics, jewelry, photography, textile, and food packaging (Cornelis et al., 2013). Discharged nanoparticles (NPs) find their way into the soils during their manufacturing, transportation, application, and disposal (Pachapur et al., 2016), and soils and aquifers act as primary filter systems to remove particulate materials from percolating water and protect water resources (Kasel et al., 2013a; Liang et al., 2013a). Many previous studies have shown the negative effects of AgNPs on human health and the environment (e.g., He et al., 2011; Carbone et al., 2014). Hence, a detailed understanding of the processes governing the transport and retention of AgNPs in soil is required to accurately assess the fate and distribution of AgNPs and to design effective strategies for reducing their toxicity in the environment.

According to the particle filtration theory, retention and mobility of NPs in porous media are controlled by physicochemical properties of both NPs and collector surfaces, such as the grain size (texture), input concentration, mineralogical composition, the presence of humic acid, the type of coatings or stabilizing agents, the solution chemistry, as well as by hydrodynamic forces (Lin et al., 2011; Liang et al., 2013a,b; Braun et al., 2015). The filtration theory has commonly been employed to describe the deposition of NPs on porous media surfaces. However, studies with NPs and natural colloids often showed deviations in predictions from filtration theory. For example, the retention of NPs may occur even under unfavorable conditions for attachment due to local surface charge heterogeneities (Lin et al., 2011), aggregation (Bradford et al., 2006), and straining in small pores and at locations of high surface roughness (Kasel et al., 2013a). Additionally, an increase in the

* Corresponding author.
E-mail address: mosaddeghi@cc.iut.ac.ir (M.R. Mosaddeghi).

https://doi.org/10.1016/j.geoderma.2018.02.016
Received 2 June 2017; Received in revised form 3 February 2018; Accepted 8 February 2018

NPs transport due to stabilizing agents causing short-range repulsive forces (El Badawy et al., 2013), retarded and asymmetric BTCs, and uniform, non-monotonic, and hyperexponential retention profiles (RPs) (Liang et al., 2013a) are examples of violations of the filtration theory.

Most researchers have studied the transport of AgNPs in highly idealized systems consisting of repacked, homogeneous, coarse-textured porous media (e.g., glass beads, quartz sands) under water-saturated or unsaturated conditions (e.g., El Badawy et al., 2013; Fang et al., 2013; Liang et al., 2013b). While these studies have provided valuable insights into the mechanisms controlling the transport of AgNPs, they do not exactly resemble natural soil conditions. Soil components such as clay minerals, organic matter, and carbonates would interact with the NPs and subsequently have a dominant effect on their fate, mobility, and potential risks to reach groundwater resources. For example, recent batch studies have shown that the retention of NPs in natural soils is correlated with the clay content (Cornelis et al., 2012). Simple porous media are not able to account for the complexity and heterogeneity (such as a wide particle size distribution, irregular grain shapes, variations in surface chemical heterogeneity, and a complex pore structure) of natural soils (Sagee et al., 2012; Liang et al., 2013a).

Unfortunately, to date, only a few column studies have focused on studying the transport of AgNPs in natural systems, leading to a serious lack of information about their fate and distribution in the environment. In natural soils, clay content and type, soil pH, the presence of organic material, and the ionic strength of the soil solution can affect mobility and bioavailability of AgNPs (Liang et al., 2013a). The information on the fate and behavior of AgNPs in soils will ultimately determine the environmental risk of AgNPs applications. Only recently, have some studies involving the transport of AgNPs in intact soil columns been conducted (Nowack and Bucheli, 2007; Sagee et al., 2012; Cornelis et al., 2013; Liang et al., 2013a; Braun et al., 2015). Neukum et al. (2014) suggested that the transport of AgNPs in sandstones is affected by the pore size distribution, mineralogy, and solution chemistry. Liang et al. (2013a) observed a significant retardation in breakthrough curves (BTCs) and hyperexponential RPs of AgNPs in natural (undisturbed) soils. Sagee et al. (2012) reported high mobility and early breakthrough of AgNPs in a disturbed sandy clay soil. They found that mechanical straining and chemical interactions between AgNPs and the soil surfaces played key roles in retention of AgNPs. Cornelis et al. (2013) suggested that straining was enhanced following fast heteroaggregation between negatively charged AgNPs and positively charged soil colloid sites and that the mobility of polyvinylpyrrolidone (PVP) coated AgNPs was significantly reduced in the natural soils. Despite the frequent existence of unsaturated water flow conditions in natural soils, information is scarcely available on the transport of NPs through unsaturated soils. Colloid retention under unsaturated flow conditions is more complicated due to the presence of air in the soil system and due to water flow being constrained to smaller pores. Colloid retention in unsaturated porous media under electrostatically unfavorable deposition conditions has been attributed to attachment to the solid–water interface (SWI), attachment to the air–water interface (AWI), deposition on solid surfaces, retention at the solid–air–water triple point and, straining in thin water films (Chen and Flury, 2005; Bradford and Torkzaban, 2008; Torkzaban et al., 2008; Fang et al., 2013; Kumahor et al., 2015). Under unsaturated conditions, colloid transport may increase due to moving AWI (McCarthy and McKay, 2004) or decrease due to greater colloid attachment to stationary AWI (Chen et al., 2008). However, most previous studies on colloid transport reported that colloid retention increased in unsaturated porous media. Bradford et al. (2002) reported that the retention of colloids under unsaturated flow conditions was controlled by the spatial distribution of water saturation and may increase due to limited preferential flow and a greater contact time between the media matrix and the colloids. Kumahor et al. (2015) also investigated the transport of citrate-coated AgNPs in unsaturated sand columns. They suggested that a non-equilibrium interaction occurred at the SWI, while an equilibrium sorption to the AWI led to retardation of AgNPs. They concluded that reversibility of attachment to the AWI was sensitive to the properties of the AWI and AgNPs, and to the solution chemistry. Moreover, Chen and Flury (2005) concluded that colloids were repelled from the AWI. Fang et al. (2013) showed that decreasing water saturation had little effect on the mobility of TiO_2 NPs through packed sand columns owing to net repulsive interactions between negatively charged AWI and TiO_2 NPs.

To the best of our knowledge, no previous study has evaluated the transport of AgNPs in calcareous soils, despite their widespread occurrence in the arid and semi-arid regions around the world. Calcareous soils contain a high amount of calcium carbonate, and Ca^{2+} bridging due to the high activity of Ca^{2+} cations may play an important role in NPs retention. Divalent cations such as Ca^{2+} and Mg^{2+} have been shown to be more effective in NPs retention than monovalent cations like Na^{+} (El Badawy et al., 2010; Liang et al., 2013a). In general, it can be expected that alkaline soils have a high potential to retain NPs compared to acidic soils because the pH value of these soils (7.0 to 8.5) is closer to the pH value at the point of zero charge (pH_{PZC}) of NPs. Also, the high Ca^{2+} concentration in calcareous soils could lead to aggregation of NPs (Hotze et al., 2010). Moreover, only a few studies have evaluated the transport and retention of AgNPs in undisturbed and/or unsaturated soil systems.

The primary objective of this research is thus to evaluate the effects of the degree of soil saturation and soil texture on the transport and retention of AgNPs in intact columns of calcareous soils. To allow for direct comparisons with previous studies, similar AgNP transport experiments were also conducted in sand columns. In addition, AgNP transport and retention data were modeled using HYDRUS-1D to better understand their transport and retention mechanisms. This information is needed to properly assess the risk of exposure of ecosystems to AgNPs and to develop strategies for waste management and remediation.

2. Materials and methods

2.1. Synthesis of AgNPs

All chemicals reagents used in our experiments were of analytical grade and were used as received without further purification. A sonochemical method was applied for preparing AgNPs in aqueous polyvinylpyrrolidone (PVP) solutions (Zhu et al., 2010). In a typical preparation, 0.05 g of PVP was added to 100 mL of aqueous solution containing 0.1 g of $AgNO_3$. The PVP acts as both reducing and capping agent. The mixture was stirred for complete dissolution and agitated under sonication. Ultrasound irradiation was carried out with a multiwave ultrasonic generator (Sonicator 3000; Bandeline, MS 72, Germany), equipped with a converter/transducer and titanium oscillator (horn), 12.5 mm in diameter, operating at 20 kHz with a maximum power output of 60 W. The operating condition was at 5 s pulse on and 5 s pulse off with amplitude of 72% at 25 °C for 20 min.

The suspension for each experiment was freshly prepared (in order to minimize the dissolution of AgNPs) by dilution of the concentrated stock suspension of stabilized AgNPs into selected electrolyte solutions to achieve an approximate concentration of 50 mg L^{-1}. The stock suspension was sonicated for 30 s with the probe before dilution. During injection into the columns, the suspension was continuously sonicated in a sonication bath.

2.2. Characterization of AgNPs

Transmission electron microscope (TEM) images of the synthesized AgNPs were obtained on a Philips CM30 instrument at an accelerating voltage of 150 kV. An average hydrodynamic diameter and surface charge characteristics of the AgNPs were determined using the Malvern ZEN 3600 Nano ZS Zetasizer (Malvern Instruments Ltd., Malvern, UK). Zeta potential (ζ) was measured with the same equipment between

−200 and +200 mV. The X-ray powder diffraction (XRD) pattern was recorded by a Philips X'Pert Pro diffractometer using CuK_α radiation to determine the crystallite size of the AgNPs. The crystallite size (D) of AgNPs was calculated using the Scherrer equation (Moore and Reynolds, 1997):

$$D = \frac{k\lambda}{\beta \cos\theta} \quad (1)$$

where k is the so-called shape factor that usually has a value of about 0.9, λ depicts the wavelength of CuK_α radiation, and β is the breadth of the observed diffraction line at half of the maximum intensity (FWHM).

2.3. Sand, soil sampling and characterization

Quartz sand with an average grain size of 264 μm and dry bulk density of 1.53 g cm^{-3} was used as an inert reference medium. To remove metal and organic impurities, the sand was washed sequentially with tap water, nitric acid (10%) and distilled water. The sand was packed into stainless steel cylinders (an inner diameter of 7 cm, a height of 15 cm, and a thickness of 2 mm).

Soil was sampled from the top 30 cm of two locations in the Isfahan Province, central Iran. The sandy loam soil (Typic Torriorthents) was sampled from the Tiran region (TR), located at 32° 40′ 20″ N 51° 13′ 46″ E, and the loam soil (Typic Haplocalcids) was sampled from the Ziar region (ZR) at 32° 30′ 57″ N and 51° 55′ 49″ E. After careful removal of possible vegetation, undisturbed soil columns were collected by using stainless steel cylinders (an inner diameter of 7 cm, a height of 15 cm, and a thickness of 2 mm) with sharpened edges. Both ends of soil-containing cylinders were then sealed with pieces of cloth.

Selected physical and chemical properties of the studied soils are given in Tables 1 and 2, respectively. Soil pH and EC values were determined in 1:2 soil:water extracts with a pH meter (CyberScan, model 2100, Eutech Instruments, Nijkerk, The Netherlands) and an EC meter (Elmetron, model CC-501, analysio GmbH, Greifswald, Germany), respectively. Soil calcium carbonate equivalent (CCE) was determined using the back-titration method (Loeppert and Suarez, 1996). Organic carbon (OC) was measured using the wet digestion method (Nelson and Sommers, 1996). Cation exchange capacity (CEC) was determined using the ammonium acetate method at pH 8.2 (Sumner and Miller, 1996). Particle size distribution was determined by the pipette method as described in Gee and Bauder (1986). Total silver concentration in the soils was determined by a PerkinElmer AAnalyst200 atomic absorption spectrometer (AAS) after open vessel aqua regia digestion (1:3 HNO3:HCl) at 140 °C (Cornelis et al., 2010).

Soil bulk density (ρ) was calculated for the intact columns according to Blake and Hartge (1986). The columns were first saturated and the saturated hydraulic conductivity (K_s) of all columns was determined using the constant-head method (Klute and Dirksen, 1986). The soil aggregate stability was characterized by the mean weight diameter (MWD) of water-stable aggregates (< 4 mm) as determined by the wet sieving method (Yoder, 1936).

2.4. Column experiments

The transport of AgNPs and bromide (Br), as an inert tracer, in the sand and undisturbed soil columns was studied. A hydrophilic nylon membrane (opening size 210 μm), as a filter, was placed at the bottom of the columns. A peristaltic pump (Longer BT100-1F, Hebei, China) with a sprinkler head was used to inject Br solutions and AgNPs suspensions at a steady flow rate (i.e., q in the range 0.03–0.70 cm min^{-1}, depending on the soil type and flow conditions) into the columns. Leaching experiments were conducted under both saturated and unsaturated flow conditions for both AgNPs and Br. The columns were first conditioned with several pore volumes of an electrolyte solution of 6 mM $Ca(NO_3)_2$ to achieve steady-state flow. Gravitational saturated flow was established by imposing a negligible pressure head on the inlet of the columns, establishing a unit hydraulic gradient and the Darcian flow rate equal to K_s. Unsaturated flow was established by controlling the inlet flow rate so that the approximate degree of saturation of 0.90 was obtained in the soil columns. Column and flow parameters for the column experiments are shown in Table 3.

Br tracer (KBr with a concentration of 10 mg Br L^{-1}, C_0) was applied to each column prior to the AgNPs transport experiments, in order to obtain flow and transport parameters. The ionic strength (IS) of the background solution was adjusted to 6 mM $Ca(NO_3)_2$ to be similar to the natural soil solution. The electrolyte solution was not buffered and pH values of the influent and effluent were in the range of 6–7. Column effluent samples were collected continuously in plastic centrifuge tubes with different increments. Br concentrations in the leachate samples were measured using an ion-selective electrode (Zhejiang Nade Scientific Instrument Co., MP523-06, Hangzhou, China) connected to a pH meter (CyberScan, model 2100, Eutech Instruments, Nijkerk, The Netherlands). Similar electrolyte solutions and flow rates were used in both Br and AgNPs transport experiments.

Suspensions of AgNPs (C_0 of 50 mg Ag L^{-1}) were injected into the columns, followed by flushing with several pore volumes of a particle-free electrolyte [$Ca(NO_3)_2$] solution. A high concentration of AgNPs was selected based on the results of batch and preliminary transport experiments, which confirmed high retention of AgNPs in these soils. Column effluent samples were collected continuously in plastic centrifuge tubes with different increments. The effluent samples were treated with concentrated HNO_3 at 175 °C for 10 min before the Ag measurement to dissolve the particles and diminish sorption onto the sampling tubes (Cornelis et al., 2010). Solutions were diluted as needed, and an Ag concentration (C) was measured by a PerkinElmer AAnalyst200 AAS (USA). Each sample was measured three times and the average value was used for further analyses. Relative concentrations (C/C_0) were plotted vs. the number of pore volumes (PV) as a breakthrough curve (BTC). The pore volume was calculated by multiplying the soil volume and the volumetric water content.

After completion of the transport experiments, the soil columns were carefully excavated in 1 cm increments (i.e., 15 layers). The total residence Ag concentration (S) in the soil columns was determined by the AAS after open vessel aqua regia digestion (1:3 HNO_3:HCl) at 140 °C (Cornelis et al., 2010). The retention profile (RP) of AgNPs was subsequently determined from this information and the measured dry mass

Table 1
Physical properties of the studied sand and soils.

Sample	Texture	Clay	Silt	Sand	ρ	MWD	d_c	K_s	φ
		kg 100 kg^{-1}			g cm^{-3}	mm	μm	cm min^{-1}	cm^3 cm^{-3}
Sand	–	–	–	–	1.53	–	264	1.700	0.420
Tiran (TR)	SL	17.8	19.9	62.3	1.52	0.41	49.0	0.032	0.425
Ziar (ZR)	L	15.7	41.5	42.8	1.20	1.29	20.4	0.080	0.544

SL - sandy loam, L - loam; d_c - median particle diameter determined using the wet sieving method, ρ - bulk density, MWD - mean weight diameter of water-stable aggregates, φ - porosity, K_s - saturated hydraulic conductivity.

Table 2
Chemical properties of the studied sand and soils.

Sample	EC	pH	CEC	OC	$CaCO_3$	K_F	N_F	Location latitude/longitude	
	$dS\,m^{-1}$		$cmol\,kg^{-1}$	$kg\,100\,kg^{-1}$	$kg\,100\,kg^{-1}$	$L\,g^{-1}$	–	N	E
	(1:2)								
Sand	0.08	7.80	0.9		–	–	–	–	–
Tiran (TR)	0.21	8.00	11.8	0.11	47.5	80.02	0.60	32.40.20	051.13.46/3
Ziar (ZR)	1.43	7.98	13.0	0.63	32.2	721.70	0.42	32.30.57	51.55.49

EC - electrical conductivity at 25 °C, CEC - cation exchange capacity, OC - organic carbon, K_F - Freundlich coefficient, N_F - Freundlich constant.

Table 3
Experimental parameters and HYDRUS-1D optimized transport parameters from Br breakthrough curves.

Sample	Degree of saturation	q_m $cm\,min^{-1}$	θ_m	q_p $cm\,min^{-1}$	θ_p	v $cm\,min^{-1}$	λ cm	R^2	SE
Sand	1	1.7	0.375	1.900	0.430	4.42	0.09	0.998	0.0019
TR soil	1	0.07	0.407	0.059	0.542	0.109	6.79	0.987	0.0157
ZR soil	1	0.09	0.453	0.081	0.450	0.181	8.46	0.982	0.0247
Sand	0.887	0.85	0.339	0.827	0.356	2.32	0.68	0.983	0.0472
TR soil	0.831	0.03	0.306	0.053	0.290	0.093	1.70	0.973	0.0176
ZR soil	0.921	0.04	0.419	0.035	0.350	0.100	6.16	0.959	0.0500

Column experiments were conducted at pH 7.0 and ionic strength (IS) = 6 mM $Ca(NO_3)_2$, q - Darcy velocity, θ - volumetric water content, $v = q_p/\theta_p$ - mean pore water velocity, λ - dispersivity. Subscripts m and p stand for measured and predicted values, respectively. R^2 - coefficient of determination, SE - standard error.

of soil in each increment.

2.5. Theory and modeling

The version 4.14 of the HYDRUS-1D software package (Šimůnek et al., 2008, 2016) was used to simulate the transport and retention of Br and AgNPs. The BTCs of a conservative tracer (Br) for each column were simulated using the equilibrium advective-dispersive equation (ADE) to inversely estimate the pore water velocity (v) and dispersivity (λ) of the undisturbed soil columns (Table 3).

Transport and retention of AgNPs in the soils were simulated using the ADE with terms representing a one-site kinetic attachment-detachment model. The aqueous and solid phase mass balance equations for AgNPs are given in this model as:

$$\theta\frac{\partial C}{\partial t} + \rho\frac{\partial S}{\partial t} = \frac{\partial}{\partial z}\left(\theta D\frac{\partial C}{\partial Z} - q\frac{\partial C}{\partial z}\right) \quad (2)$$

$$\rho\frac{\partial S}{\partial t} = \theta k_{att}\psi C - k_{det}\rho S \quad (3)$$

where θ [−] is the volumetric water content, t [T, T denotes time units] is time, C [N_cL^{-3}, N_c and L denote the number of NPs and units of length, respectively] is the aqueous phase AgNPs concentration, ρ [ML^{-3}, M denotes mass units] is the soil bulk density, S [N_cM^{-1}] is the solid phase AgNPs concentration, z [L] is the distance from the column inlet, D [L^2T^{-1}] is the hydrodynamic dispersion coefficient, q [LT^{-1}] is the Darcian water flux, k_{att} [T^{-1}] is the first-order attachment coefficient, k_{det} is the first-order detachment coefficient, and ψ [−] is a dimensionless function to account for time- and depth-dependent blocking given as (Bradford et al., 2006):

$$\psi = \left(1 - \frac{S}{S_{max}}\right)\left(\frac{d_c + z}{d_c}\right)^{-\beta} \quad (4)$$

where d_c [L] is the median diameter of soil grains, β [−] is an empirical parameter, which controls the shape of the retention profile of NPs (i.e., the depth dependence of the retention coefficient), and S_{max} [N_cM^{-1}] is the maximum solid phase concentration of deposited AgNPs. Eq. (4) can account for time- and depth-dependent retention and can produce retention profiles which can be exponential, uniform, or hyperexponential with depth (Kasel et al., 2013a).

The first term on the right side of Eq. (4) accounts for time-dependent blocking/filling of attachment sites based on Langmuirian dynamics (Liang et al., 2013a). This model indicates that retention decreases with time as the attachment sites are gradually being filled with NPs and the retention profile becomes uniform with depth as S approaches S_{max}. When S_{max} is large, the blocking term approaches unity and the decrease in retention with time is not considered (Kasel et al., 2013a). The second term on the right side of Eq. (4) accounts for depth-dependent retention.

Similarly to Kasel et al. (2013a), four different model formulations for blocking were considered in our study: Model 1 (M_1) is the conventional attachment and detachment model ($\psi = 1$); Model 2 (M_2) when $\beta = 0$ includes attachment, detachment, and Langmuirian blocking; Models 3 (M_3) and 4 (M_4) when $\beta > 0$ additionally also consider depth-dependent retention, producing retention profiles of AgNPs, which exhibit a hyperexponential shape (e.g., a higher deposition rate close to the column inlet). Liang et al. (2013a,b) used optimal values of $\beta = 0.432$ and $\beta = 1.532$ for simulations of the AgNPs transport in sand and soil, respectively. However, these β values did not adequately describe the shape of the observed depth-dependent retention profiles in our study. Therefore, we used $\beta = 0.765$ based on information presented in the literature (Kasel et al., 2013a). In M_3, S_{max} was set to a large value so that the first term on the right side of Eq. (4) is approximately equal to 1. In M_4, S_{max} was set equal to a value that resulted in the first term on the right side of Eq. (4) smaller than 1.

The AgNPs retention model parameters (k_{att} and S_{max}) were optimized by simultaneously fitting the experimental BTCs and RP data using HYDRUS-1D. The pore water velocity (v) and dispersivity (λ) were fixed at values optimized using the Br BTCs. The coefficient of linear regression (R^2), Akaike Information Criterion (AIC), root mean square error (RMSE), and standard error (SE) were used to evaluate the modeling efficiency. The AIC was calculated using the following equation (Akaike, 1998):

$$AIC = 2K + N\ln\left(\frac{RSS}{N}\right) \quad (5)$$

where K is the number of adjustable parameters in the model, N is the number of data points to be fitted, and RSS is the residual sum of

squares.

The Peclet number (P_e), a measure that characterizes the ratio of advective transport to diffusive transport, was calculated using the following equation (Tufenkji and Elimelech, 2004):

$$P_e = \frac{vL}{D} \quad (6)$$

where D (L^2T^{-1}) is the hydrodynamic dispersion coefficient and L is the soil column length.

The following equation was used to determine the filtration coefficient (λ_f, m^{-1}) (Matthess et al., 1988):

$$\lambda_f = \ln\left(\frac{\overline{C_{influent}}}{\overline{C_{effluent}}}\right) \times \frac{1}{L} \quad (7)$$

where $\overline{C_{influent}}$ and $\overline{C_{effluent}}$ represent the average influent and effluent concentrations over the leaching time (N_cL^{-3}) and L is the sampling depth (L), which is equal to the soil column length. The $\overline{C_{influent}}$ and $\overline{C_{effluent}}$ concentrations were determined using the numerical integration of influent (C_0) and effluent (BTC) concentration curves.

3. Results and discussion

3.1. Characterization of AgNPs

Fig. 1b illustrates the XRD pattern of the synthesized AgNPs. The XRD pattern of the AgNPs showed diffraction peaks at 2θ = 38, 44, 64, and 77 assigned to (111), (102), (110) and (120) planes, respectively, of a faced centered cubic (FCC) lattice of silver (Majeed Khan et al., 2011). The average size of the synthesized AgNPs, calculated from the XRD pattern by the Scherrer equation (Eq. (1)), was around 29 nm. The TEM images of AgNPs revealed that the average size was about 40 nm (Fig. 1a). The Z-average hydrodynamic diameter of the AgNPs was 157.59 nm, as measured by DLS, and the zeta potential (ζ) value was close to neutral (−2.7 mV). The size obtained by DLS is considerably larger than that determined by XRD and TEM, which can be explained by the predominant contribution of the large particles or aggregates on the light scattering signal and by the fact that DLS measures not only the size of the NPs, but also the additional layer corresponding to the solvent moving together with the particles (Ito et al., 2004).

3.2. Transport of bromide through saturated and unsaturated columns

Fig. 2 presents the observed and simulated BTCs of Br under both saturated and unsaturated flow conditions in the sand and soil columns. The classical ADE, Eq. (2), well describes the BTCs of a conservative tracer under both saturated and unsaturated flow conditions (R^2 = 0.99 and 0.98, respectively). Therefore, Br transport parameters accurately characterize the physical conditions of leaching experiments. The modeled and measured hydraulic parameters and dispersivity values of the repacked quartz beads and undisturbed soil columns are given in Table 3.

The transport of Br, as an inert tracer, is not affected chemically and its BTCs should depend only on physical processes in the porous media. The Br BTCs have steep increases and decreases of concentrations and are approximately symmetric in shape (Fig. 2a), indicating that physical non-equilibrium is not significant for the Br transport in the sand column experiments due to a narrow pore size distribution of the sand. Although the physical non-equilibrium model can provide a better description to the Br BTCs than the simple ADE model in unsaturated sand and intact soils columns, we decided to use the ADE model due to its simplicity. Fig. 2b and c show that in the intact soils, the Br BTCs deviated from the symmetrical shape and shifted to the left relative to the equilibrium transport curve. In contrast to the sand columns, Br was detected in the first collected volume of the effluent from the intact soil, which suggests the existence of preferential flow (Dousset et al., 2007). The BTC for the TR soil shows a less diffuse front compared to that for the ZR soil, which is characterized by a more gradual increase of Br concentrations to C/C_0 = 1 before 3PV. The breakthrough of Br in the ZR soil columns shows a sharp front between 3PV and 4PV (Fig. 2c).

The BTCs were more symmetrical in saturated than in unsaturated sand columns (Fig. 2a). Similar to the literature (e.g., Torkzaban et al., 2008), the dispersivity values were greater for unsaturated conditions than for saturated conditions in the sand columns. Although considerable differences between saturated and unsaturated conditions were not observed in soil columns, the dispersivity values were greater for saturated conditions (Table 3). The BTC under saturated conditions in the TR soil exhibits more asymmetry and early appearance of Br in the effluent (Fig. 2b). This behavior indicates that Br was transported relatively rapidly by a small fraction of the total soil water (bypassing the soil matrix). Similar results were reported by Seyfried and Rao (1987) in undisturbed soil columns, who suggested that under unsaturated conditions, conducting pore sequences do not contribute to the transport processes, which results in the reduction of the asymmetry in BTCs and in compressing the solute front in undisturbed soil columns. Moreover, Bradford et al. (2004) suggested that the asymmetric shape (early appearance, tailing, and approach to the peak effluent concentration) of the Br BTCs is controlled by the degree of bypassing water. However, in the ZR soil, saturation conditions had a negligible effect on the Br BTCs. These differences could be explained by the structural heterogeneity in this soil. The pore network in the ZR soil is likely sufficiently interconnected so that drainage of large pores cannot disconnect the conducting pore sequences.

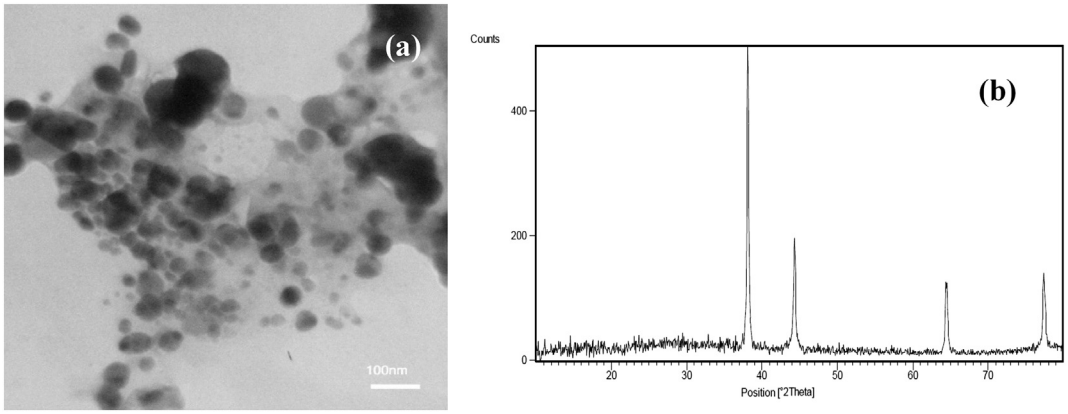

Fig. 1. (a) Transmission electron microscopy (TEM) images and (b) X-ray diffraction (XRD) patterns of the synthesized silver nanoparticles (AgNPs).

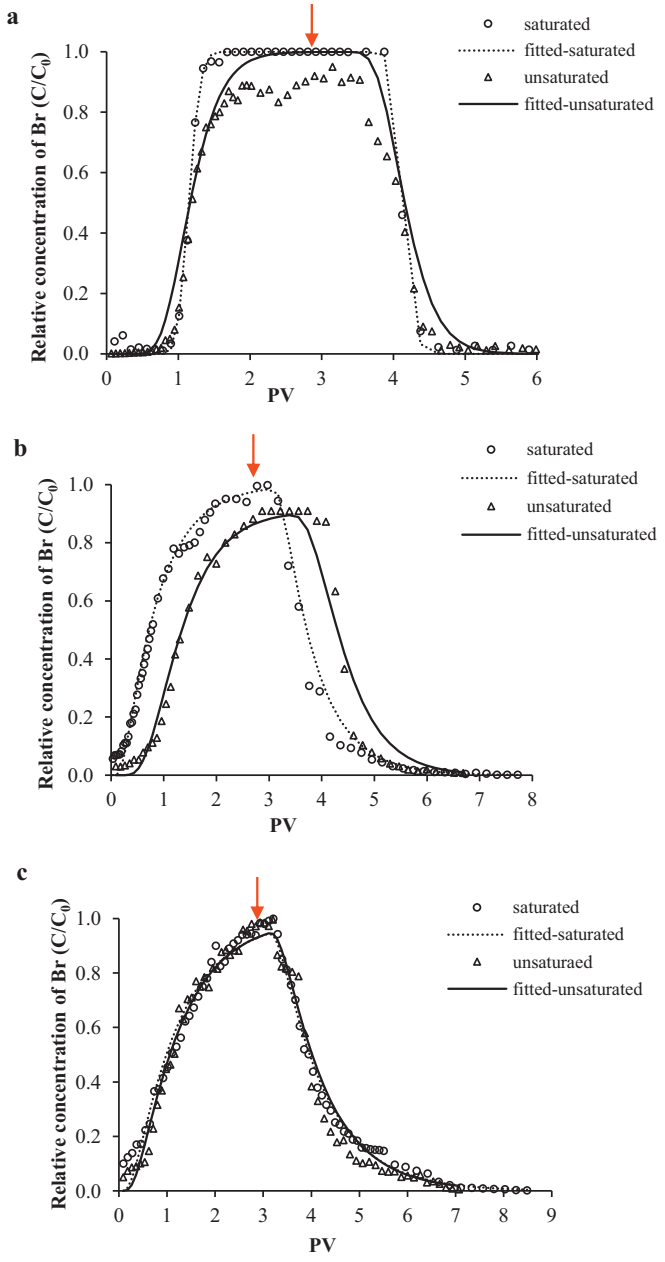

Fig. 2. Observed (dots) and fitted (lines) BTCs of Br tracer in (a) sand, (b) TR soil, and (c) ZR soil columns under saturated and unsaturated flow conditions (PV is the number of pore volumes). The arrow indicates the end of the tracer pulse. Continuous curves represent the HYDRUS-1D simulations using the equilibrium advective-dispersive equation (ADE).

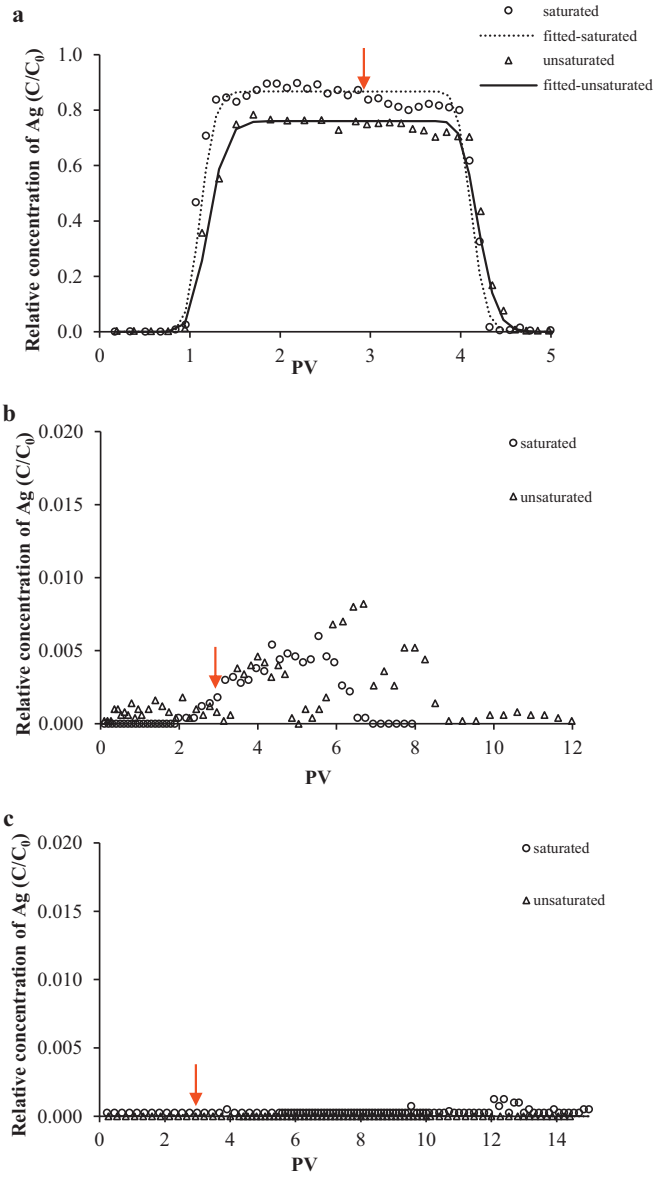

Fig. 3. Observed and simulated breakthrough curves for silver nanoparticles in (a) sand columns, and observed breakthrough curves for AgNPs in (b) TR soil, and (c) ZR soil columns (PV is the number of pore volumes). The background electrolyte was 6 mM Ca $(NO_3)_2$ and the AgNPs input concentration was 50 mg L^{-1}. The arrows indicate the end of the AgNPs pulse. Continuous curves represent the HYDRUS-1D simulations using the one-site kinetic attachment-detachment model (Model 1, M1). Note different vertical scales in the graphs.

3.3. Transport and retention of AgNPs through saturated and unsaturated columns

Fig. 3 presents the observed and simulated BTCs of AgNPs under both saturated and unsaturated conditions in the sand columns (Fig. 3a) and observed BTCs of AgNPs in soil columns (Fig. 3b,c). Furthermore, retention profiles (RPs) of AgNPs for the undisturbed soil columns for both flow conditions are illustrated in Fig. 4. The BTCs are plotted using normalized concentrations (C/C_0) of AgNPs as a function of the number of pore volumes (PV) and RPs are plotted using normalized solid phase concentrations (S/C_0) as a function of depth. In the sand columns, around 85%–90% of AgNPs were transported through the columns and recovered in the effluent. We believe that 10%–15% of AgNPs were retained in the sand columns, which cannot be measured accurately. Because of considerable differences between model parameters for two replications of natural soil columns, each soil column replicate has been considered as a separate sample. Other studies, such as those by Cornelis et al. (2013) and Sagee et al. (2012), also reported similarly large variations between natural soil columns.

In both saturated and unsaturated sand columns, AgNPs are first detected in the effluent when PV < 1. Afterward, the C/C_0 values increased sharply and reached a plateau close to values of 0.9 and 0.8 at PV = 1 in the saturated and unsaturated columns (Fig. 3a), respectively. This suggests that the deposition rate of AgNPs is not affected by the concentration of deposited AgNPs on the sand grain surfaces. The effluent (M_{eff}), sand or soil column (M_{soil}), and total ($M_{total} = M_{eff} + M_{soil}$) mass recoveries of AgNPs are shown in Table 4. The mass recoveries of AgNPs in both saturated and unsaturated sand columns are > 84% (i.e., 88.9 and 84.9 for saturated and unsaturated

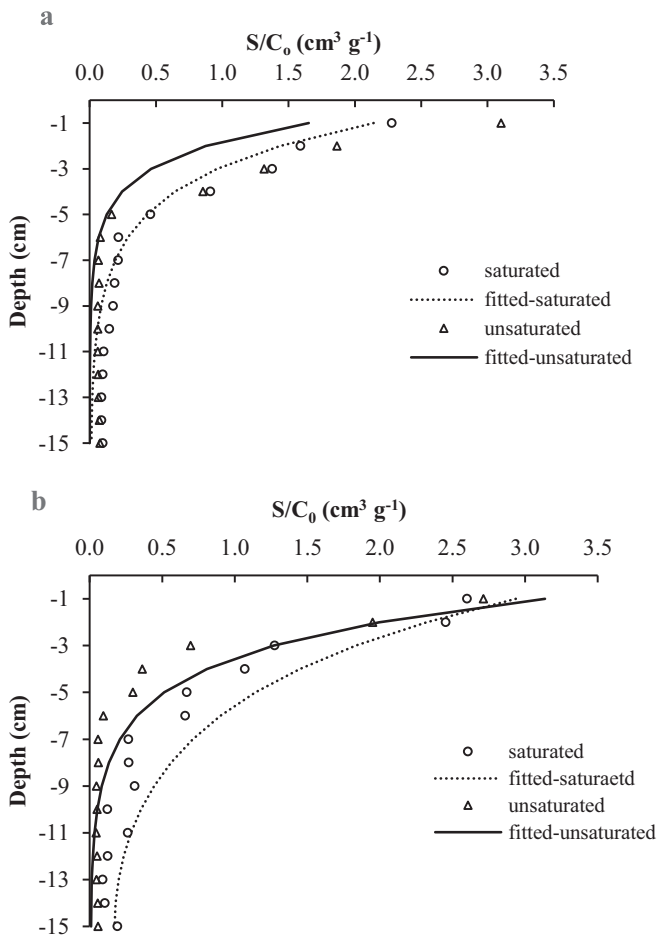

Fig. 4. Observed and simulated retention profiles for silver nanoparticles in (a) TR and (b) ZR soil columns. The background electrolyte for leaching experiments was 6 mM Ca $(NO_3)_2$ and the AgNPs input concentration was 50 mg L^{-1}. The arrows indicate the end of the AgNPs pulse. Continuous curves represent the HYDRUS-1D simulations using the one-site kinetic attachment-detachment model, in which blocking is combined with depth-dependent retention (M4).

Table 4
Mass recoveries of AgNPs, filtration coefficients, and Peclet numbers in the sand and soil columns under saturated and unsaturated conditions.

Flow conditions	Sample	M_{eff}	M_{soil}	M_{total}	λ_f	P_e
		%	%	%	m^{-1}	
Saturated	Sand	88.90	ND	88.90	0.86	170.84
	TR soil-1	0.60	99.20	99.80	34.47	2.21
	TR soil-2	0.02	95.30	95.32	26.17	2.66
	ZR soil-1	0.70	89.80	90.50	32.91	1.77
	ZR soil-2	0.20	98.80	99.00	40.10	1.50
Unsaturated	Sand	84.90	ND	84.90	0.85	22.16
	TR soil-1	1.10	99.00	100.10	28.11	7.50
	TR soil-2	0.01	94.30	94.31	30.85	6.00
	ZR soil-1	0.10	99.10	99.20	46.63	2.43
	ZR soil-2	0.10	60.90	61.00	43.78	1.33

M_{eff}, M_{soil}, and M_{total} are mass percentages recovered from effluent, soil/sand samples, and total (sum of both), respectively; ND - not detected. λ_f - filtration coefficient, $P_e = vL/D = L/\lambda$ - Peclet number, where v is the mean pore water velocity, L is the length of the columns (=15 cm), and D is the hydrodynamic dispersion coefficient ($D = \lambda v$, λ is dispersivity).

conditions, respectively, see Table 4), suggesting low retention in the sand columns. This is consistent with other studies, indicating that the sand surfaces are unfavorable for particle deposition (Fang et al., 2013). Straining is also unlikely to be involved in the retention of AgNPs in sand beads because of the small size of AgNPs and a low d_p/d_c value (i.e., 0.0009), where d_p [L] is a diameter of the particles and d_c [L] is the median grain diameter of the collector. However, the low retention is probably attributed to other retention mechanisms such as chemical heterogeneity of colloids, surface charge heterogeneity on the sand grains, surface roughness, colloid aggregation, and enhanced colloid retention in low-velocity regions (Fang et al., 2013).

The results show that the BTCs obtained under unsaturated conditions exhibit the same behavior as those under saturated conditions in the sand columns (Fig. 3a). The peak effluent concentration of AgNPs under unsaturated conditions is lower than under saturated conditions (Fig. 3a). Bradford et al. (2006) discussed that the colloid-accessible fraction of the pore space decreases with decreasing water saturation. Furthermore, the unsaturated hydraulic conductivity rapidly decreases with decreasing water saturation. Hence, the retention forces acting on the attached colloids in unsaturated systems are expected to be stronger than in saturated systems (Bradford and Torkzaban, 2008; Torkzaban et al., 2008).

Small fluctuations in AgNP concentrations were observed at some parts of BTCs (Fig. 3) for both soil and sand columns. Although other authors such as Kasel et al. (2013a) and Kumahor et al. (2015) also observed such fluctuations, no acceptable explanation has been suggested so far.

Fig. 3b and c present the BTCs for AgNPs in the TR and ZR soils, respectively. Nearly all AgNPs introduced into both soils were retained in the soil columns. Percentages of AgNPs leached out of the ZR and TR soil columns were < 1% of the injected total mass and the averages of the total column mass recoveries of AgNPs in the soil columns were in the range of 90–100% (except for the unsaturated ZR soil-2 column, see Table 4). This finding indicates the accuracy and correctness of our experimental procedures and protocols.

In the ZR soil, effluent concentrations of AgNPs from the saturated and unsaturated soil columns were around the detection limit of AAS during the entire experiments and no noteworthy breakthrough could be observed (Fig. 3c). In the TR soil under saturated conditions, AgNPs appeared in the effluent after 2.5 PV and their concentrations gradually increased to a maximum C/C_0 of 0.005 after 5 PV (Fig. 3b). Following the reintroduction of AgNP-free solutions, the effluent concentrations of AgNPs declined, approaching zero at approximately 7 and 9 PV under saturated and unsaturated conditions, respectively.

Similar results have been reported by other researchers. Braun et al. (2015) reported that no breakthrough of AgNPs occurred in the silty loam soil at a flow velocity of 0.0015 cm min^{-1} due to high retention and that the RPs were strongly hyperexponential, compared to the exponential distribution of AgNPs in the loamy sand soil. Cornelis et al. (2013) observed high retention and small effluent concentrations of AgNPs in 11 natural soil columns. Kasel et al. (2013b) also observed almost complete retention of functionalized multi-walled carbon nanotubes (MWCNT) in two undisturbed soils at water contents close to saturation (i.e., degree of saturation of 85–96%). They recovered > 86% of MWCNT in the soil profile and their experiments showed no detectable breakthrough of MWCNT. Several reasons have been mentioned to explain the high retention of NPs in natural soils: sedimentation and straining of NPs on soil minerals following their aggregation and/or heteroaggregation (Cornelis et al., 2013), physical filtration mechanisms (Kasel et al., 2013b), grain size effects, mineralogical composition of the soil or long-term colloidal stability of NPs (Braun et al., 2015; Sagee et al., 2012), nanoscale chemical and physical heterogeneity on the soil surfaces and blocking effects (Liang et al., 2013a), and attachment mechanisms (Bradford et al., 2004). It is reported that soil colloids containing Fe, Al, and Si (Liang et al., 2013a; Neukum et al., 2014) could provide favorable attachment sites for AgNPs.

The surfactant coatings on the AgNPs can also affect the retention of AgNPs. Lin et al. (2012) investigated the efficiency of AgNPs with two different polymer coatings (poly vinylpyrrolidone or Arabic gum) to

aggregate and deposit on a silica surface. They reported that polymeric coatings could not necessarily stabilize AgNPs against deposition unless the collector surfaces are also coated with the polymer. The lower mobility of AgNPs in the soil columns compared to the sand columns can be explained by a high ratio of the surface area to the volume of the fine-grained soils, the mechanical straining of AgNPs, or by the enhanced availability of favorable attachment sites (Braun et al., 2015). Moreover, repulsive interactions arising from the surfactant on the AgNPs were more pronounced in the sand medium than in natural soils (Liang et al., 2013a).

The transport of AgNPs was highly retarded in comparison with the inert tracer (Br) in the TR soil (see Figs. 2b and 3b). The similar retardation-type behavior of engineered NPs has been previously reported (Torkzaban et al., 2010; Liang et al., 2013a; Kumahor et al., 2015). Torkzaban et al. (2010) reported delays in the breakthrough of quantum dot NPs (QDNPs) due to high initial rates of particle deposition. They suggested that a high diffusive mass transfer rate of QDNPs from the bulk solution to the sand surfaces and the QDNPs mass transfer to the unfavorable regions of the sand surfaces can explain this behavior. Also, coatings of the natural organic material (NOM) may result in more hydrophobic AgNPs in soil (Kumahor et al., 2015). Hence, a reversible attachment process would occur and the BTCs would be observed with retardation.

Our results indicated that despite significant differences in dispersivities and porosities between the two studied soils (see Table 3), > 90% of AgNPs were recovered in the RPs of these soils and shapes of RPs were very similar (Fig. 4). In fact, the AgNPs retention in the ZR soil was slightly stronger than in the TR soil, which may be attributed to the smaller grain sizes and higher electrical conductivity of the ZR soil (see Table 1). Bradford et al. (2002, 2004) also reported a decreasing trend in effluent colloid concentrations and increasing colloid retention in heterogeneous systems with decreasing median grain size (d_{50}).

In general, the higher retention of AgNPs in the soil columns compared to the sand columns can be attributed to the properties of the soils, such as the presence of NOM, greater surface charges, and a wider particle size distribution. Liang et al. (2013a,b) also observed lower effluent concentrations in a soil with smaller d_{50} in comparison to sand. They suggested that soil heterogeneity decreased the energy barrier for NP aggregation in comparison to the same homogeneous situation. Filtration theory provides an explanation for this behavior because it predicts that with a decrease in the grain size (or an increase in the specific surface area), the mass transfer rate to the collector surface is expected to increase (Liang et al., 2013a; Braun et al., 2015). Additionally, the presence of NOM and calcium carbonate in the alkaline soils may have a stabilizing or destabilizing effect on the AgNP retention in natural soils compared to sand. The soil organic matter exists as solid particles (humins) or as dissolved compounds in the soil solution (fulvic and humic acids). Electrostatic attraction due to variable charges on NOM surfaces can effectively adsorb charged NPs (Peralta-Videa et al., 2011), which can remove NPs to the solid phase. On the other hand, the dissolved organic matter in soil may be sorbed on NPs surfaces and through charge alteration (reduction in the pH_{PZC}) or steric forces may increase hydrophilicity of the surfaces (Espinasse et al., 2007), which may decrease aggregation of NPs and increase their mobility in natural soils (Peralta-Videa et al., 2011). However, due to the lack of information on the properties of NOM in the studied soils, their specific contributions to the retention of AgNPs cannot be predicted.

Pore-water chemistry can affect the mobility of AgNPs in soils (El Badawy et al., 2010). The high activity of Ca^{2+} cations probably plays an important role in AgNPs retention in the calcareous soils. Retention of AgNPs is enhanced at higher IS due to compression of the electrostatic double layer and a decrease in the magnitude of the surface potentials of both NP and collector surfaces (Bradford et al., 2006). Previous studies have demonstrated that deposition phenomenon enhanced with an increase in IS or cation valence due to heteroaggregation, and homoaggregation had a negligible effect (Cornelis et al., 2013; Liang et al., 2013a; Braun et al., 2015).

In calcareous soils, the AgNPs transport may be affected by surface interactions with the carbonates. Moreover, our previous experiments that were conducted in a batch system for nine different calcareous soils (Rahmatpour et al., 2017) suggested significant and positive correlations between sorption isotherm parameters of AgNPs and pH due to the increased hydrolysis/precipitation of Ag^{+} ions released from the PVP-AgNPs. In addition, using electrolyte solution [i.e., 6 mM Ca $(NO_3)_2$] and the presence of Ca^{2+} in solution could affect the AgNPs behavior in our transport experiments. The results of Braun et al. (2015) indicated that the presence of Ca^{2+} affected AgNPs transport even at low concentration (i.e., 1 mM). The divalent cation Ca^{2+} could affect the AgNPs transport by creating nanoscale chemical heterogeneity on the solid surfaces that can neutralize or reverse the surface charges at specific locations (Bradford et al., 2015) and/or can induce cation bridging between functionalized NPs and negatively-charged sites on the clay surfaces (Liang et al., 2013a).

Hyperexponential retention profiles (RPs) were observed in both soils (Fig. 4). Retention of AgNPs decreased gradually along the travel distance, with a maximum concentration of 100–130 mg kg^{-1} near the column inlet and a minimum solid-phase concentration of 5 mg kg^{-1} near the column outlet. The higher concentration of AgNPs near the column inlet in ZR soil columns in comparison with TR soil columns (Fig. 4) can be related to higher EC (Table 2) and greater divalent cations (data not shown) in ZR soil. Similarly Zhang et al. (2017) reported more retention of MWCNT in the presence of Ca^{2+} compared with K^{+} ions. They also observed that in the presence of Ca^{2+}, the blocking behavior enhanced and RPs exhibited a hyperexponential shape. In fact, after leaching of the columns with distilled water for 20 pore volumes, the percentages of input AgNPs retained in the soils are > 90% in both soils. A significant fraction of retained AgNPs (approximately 90%) is recovered in the top 0–4 cm (Fig. 4). Bradford et al. (2004) suggested that the number of dead-end pores decreases with increasing distance, which results in the colloid transport occurring mainly within the large pores and bypassing smaller pores due to limited transverse dispersivity or size exclusion. Surface roughness and straining at grain-grain contacts, chemical heterogeneities on colloid surfaces, nanoparticle aggregation (Kasel et al., 2013a), hydrodynamic forces, and variations in the pore-scale velocity (Liang et al., 2013a) can provide a viable explanation for hyperexponential RPs in the soil columns. The physical blocking of NPs in dead-end pores or straining of NP heteroaggregates are other possible explanations for retention of NPs in soil columns (Cornelis et al., 2013). Straining is also suggested to be a process that can explain hyperexponential retention profiles (Fig. 4) when most AgNPs are retained in the upper first centimeters of the columns. However, straining is more important for relatively large particles or aggregates with larger drag coefficients (Bradford and Torkzaban, 2008).

The BTCs of AgNPs for saturated and unsaturated columns show no significant difference and they almost overlap (Fig. 3). Fang et al. (2013) also reported that the presence of air under the unsaturated conditions had only a limited effect on the transport of TiO_2 NPs at low IS. The light microscope observations of Chen and Flury (2005) indicated that colloids did not adhere to the air–water interface under unsaturated conditions. Moreover, in the current study, the large hydrodynamic diameter of AgNPs (i.e., 157.59 nm) in comparison with the thickness of the thin water film (~50 nm) during steady-state water flow conditions (Torkzaban et al., 2008) excluded the possibility of film straining under unsaturated conditions as suggested by Fang et al. (2013).

The filtration coefficients (λ_f) and the Peclet numbers (P_e) are also presented in Table 4. It is expected that much larger λ_f values should be observed in natural soil columns compared with the homogenous sand columns. The key role of soil structure and texture in the transport and retention of particles has been demonstrated in several studies (e.g.,

Safadoust et al., 2011). However, in our study, λ_f is not significantly affected by soil texture and saturation conditions (Table 4). Under saturated conditions, the λ_f values are larger in the ZR soil than in the TR soil (an average of two replications; 30.32 ± 5.87 and 36.50 ± 5.08 m^{-1} for the TR and ZR soils, respectively). Under unsaturated flow conditions, a similar trend is observed (an average of two replications; 29.48 ± 1.50 and 45.21 ± 1.94 m^{-1} for the TR and ZR soils, respectively). It seems that the potential for a larger contact of AgNPs with soil particles and adsorption sites helps to explain the larger values of λ_f in the ZR soil columns. As mentioned above, the greater EC could also increase the filtration coefficients as well as more retention sites were present in this soil. Moreover, slight differences are observed among the λ_f data for the two flow conditions in the ZR soil. The averaged λ_f under unsaturated flow conditions (45.21 ± 1.94 m^{-1}) is larger than under saturated flow conditions (36.50 ± 5.08 m^{-1}) in the ZR soil. However, this difference is negligible in the TR soil (30.32 ± 5.87 and 29.48 ± 1.94 m^{-1}, respectively). This tiny difference in sandy loam soil may be explained by a weak structure or the occurrence preferential flow in this soil.

The pore water velocity is an important factor affecting the NP filtration in soils. A significant power relationship was derived between the filtration coefficient (λ_f) and the pore water velocity (v) using all data (Fig. 5). The relation indicates that as the average pore water velocity increases, AgNPs filtration decreases, which is in agreement with Safadoust et al. (2011) who reported that the filtration coefficient for *E. coli* in soil columns increased as a result of a reduced flow rate. The data points in Fig. 5 may be divided into two groups; a group which corresponds to data for natural soils and another one (with very low λ_f values) which corresponds to data for sand. The nonlinear relation can also be represented by two linear relations if we consider the two groups separately. In other words, a linear relation between λ_f and v for the soil columns would have a much greater slope than for the sand columns, indicating that the pore water velocity has a dominant effect on the AgNPs transport through natural soils.

The Peclet number (P_e) indicates a relative importance of the mass transport (advection) in comparison with diffusion (see Eq. (6)). According to the filtration theory, the dominant mass transfer process for particles smaller than 1 μm is the diffusion process (Braun et al., 2015). Generally, P_e decreases faster with a decrease in the grain size and water content (Table 4). For instance, P_e decreased from 170 for the sand columns to 2.4 and 1.6 for the TR and ZR soil columns in saturated flow conditions, respectively. The corresponding P_e values for unsaturated flow also decreased from 22 for the sand columns to 6.7 and 1.9 for the TR and ZR soil columns, respectively. These results indicate

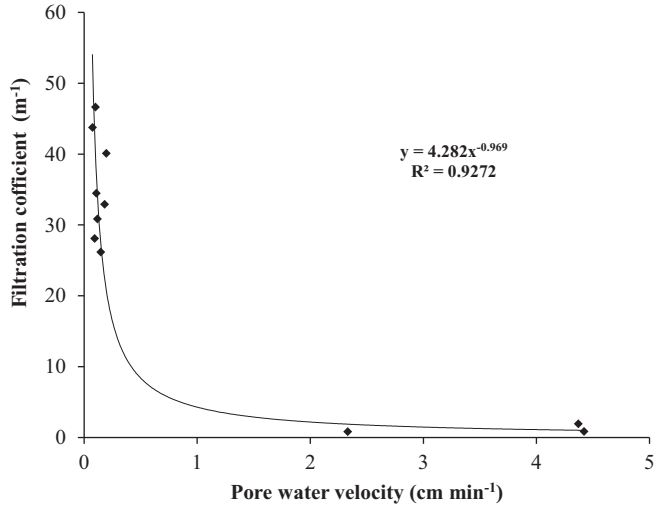

Fig. 5. Overall relationship between the filtration coefficient (λ_f) and the pore water velocity (v).

that for the sand columns the role of diffusion/dispersion relative to advection is much more significant under unsaturated conditions. Braun et al. (2015) suggested that an increased deposition of AgNPs at low flow rates is related to an increasing impact of diffusion because some soil pores are empty and the ability of soil to conduct water decreases. It seems that for undisturbed soils, saturation conditions have no remarkable effect on the P_e value (Table 4). This may be due to near-saturated conditions used in this study.

3.4. Modeling AgNP transport and retention in saturated and unsaturated columns

Four models (M_1 to M_4) based on the original attachment-detachment model were fitted to the AgNP transport (BTCs) and retention (RPs) data. Table 5 summarizes the values of the fitted parameters for models M_1, M_2, M_3, and M_4, as well as statistical indices indicating the goodness of fit such as the coefficient of determination (R^2), RMSE, and AIC. The AIC (Eq. (5)) is a criterion to select the best model with the lowest RSS and the lowest number of fitting parameters (i.e., K); the best model is the model with the smallest AIC. All four model formulations (M_1, M_2, M_3, and M_4) described the AgNPs transport and retention quite well with $R^2 > 0.80$ (Table 5).

A good agreement between measured and modeled BTCs was obtained using the M_1 model (i.e., a conventional attachment-detachment model) for the sand columns. However, the BTCs for the natural soil columns were not successfully simulated using the M_1 model because of favorable deposition sites in the soils with high clay and calcium carbonate contents (Table 1). Also, for undisturbed soil columns, a decrease in the colloid concentration with depth simulated with the M_1 model was generally steeper than that shown by the experimental data.

The smallest AIC values for soil columns were obtained for the M_2 or M_4 models (Table 5), indicating that the models that included the Langmuirian blocking term provided the best agreement with the observed data. However, since experimental RPs were hyperexponential with distance, indicating that the retention coefficient exhibited a depth-dependency, and since large values of SE were observed for the M_2 parameters, it is unlikely that this model (i.e., M_2) is the best model for simulating the AgNPs behavior in the soil columns. The improved description may be attributed to the increased flexibility (i.e., more adjustable parameters) of the M_2 model as also mentioned by Bradford et al. (2003).

The M_3 model described the experimental data (BTCs and PRs) fairly well. However, some deviations were observed between the experimental and simulated RPs. Model M_3 tended to underestimate the high concentrations near the column inlet. On the other hand, with the exception of the second saturated columns of the ZR soil, the smallest R^2, and highest RMSE were obtained using this model.

Finally, since model M_4 includes a depth-dependency in the retention coefficient, the spatial distributions of colloids were more consistent with the M_4 simulations than with the other models when both BTCs and RPs were considered. The values of R^2 for the M_4 model were larger than 0.92 (see Table 5).

Modeling of each replication of a particular soil column experiment indicates that the transport parameters are highly variable (Table 5). However, high retention of NPs in all replications is pronounced (see Table 4 and Fig. 4). Cornelis et al. (2013) also reported highly variable transport parameters and mass recoveries for AgNPs in natural soil columns. Greater physical and chemical heterogeneities of intact soil columns (i.e., a pore size distribution and pore continuity) could explain such variability compared to homogenous sand columns (Table 5).

Symmetrical BTCs of AgNPs for the sand column experiments under both saturated and unsaturated flow conditions, in which no data was available on RPs, could be best fitted using the conventional attachment-detachment model (M_1) (R^2 of 0.987 and 0.972, respectively) (see Fig. 3a and Table 5). Accordingly, other researchers also reported good

Table 5
Parameters obtained by fitting different transport models to the experimental AgNPs breakthrough curves and retention profiles using HYDRUS-1D.

Flow conditions	Sample	Model	RMSE	AIC	R^2	β	k_{att} / h^{-1}	SE k_{att}	S_{max}/C_0 / $cm^3\,g^{-1}$	SE S_{max}/C_0
Saturated	Sand	M1	0.0165	−417.7	0.987		4.30×10^{-2}	0.33×10^{-2}		
	TR soil-1	M1	0.180	−222	0.983		52.96	4.21		
	TR soil-2	M1	0.0842	−271.3	0.960		11.36	2.96		
	ZR soil-1	M1	0.028	−725	0.959		7.328	0.456		
	ZR soil-2	M1	0.0264	−1133	0.922		12.41	0.819		
	Sand	M2	0.0183	−405.1	0.984		0.042	0.36×10^{-2}	2596.2	3.62×10^{-14}
	TR soil-1	M2	0.037	−425	0.968		110.14	33.53	5.88	0.724
	TR soil-2	M2	0.082	−271	0.965		25.50	13.73	2.50	0.813
	ZR soil-1	M2	0.013	−1358	0.983		123.92	11.35	3.043	0.04
	ZR soil-2	M2	0.0298	−713.5	0.956		5.78	0.403	$1.0 \times 10^{+5}$	$4.11 \times 10^{+7}$
	Sand	M3	0.0185	−406	0.983	0.765	0.399	0.13		
	TR soil-1	M3	0.954	−506	0.940	0.765	338.72	990.11		
	TR soil-2	M3	0.137	−218	0.849	0.765	689.7	244.89		
	ZR soil-1	M3	0.0729	−533.2	0.887	0.765	637.51	371.35		
	ZR soil-2	M3	0.062	−864.9	0.841	0.765	628.19	536.14		
	Sand	M4	0.017	−414.4	0.986	0.765	1.53	0.12	$0.33 \times 10^{+6}$	0.34×10^{-18}
	TR soil-1	M4	0.0151	−542.3	0.986	0.765	4013.4	288.67	11.33	0.423
	TR soil-2	M4	0.0829	−270.9	0.961	0.765	3026.4	1285.3	2.085	0.245
	ZR soil-1	M4	0.024	−755.1	0.964	0.765	1633.5	140.57	3.59	0.227
	ZR soil-2	M4	0.0249	−1148	0.921	0.765	2839.5	304.25	182.49	9.799
Unsaturated	Sand	M1	2.16×10^{-2}	−459.2	0.973		1.15×10^{-2}	0.28×10^{-2}		
	TR soil-1	M1	0.062	−416	0.975		7.35	2.85		
	TR soil-2	M1	0.055	−433	0.937		8.69	2.494		
	ZR soil-1	M1	0.028	−671	0.972		11.35	0.858		
	ZR soil-2	M1	0.017	−761	0.973		9.21	0.509		
	Sand	M2	0.023	−449	0.976		5	2.286	0.765	0.239
	TR soil-1	M2	0.052	−440.2	0.936		35.22	19.36	2.02	0.204
	TR soil-2	M2	0.041	−475.2	0.969		76.47	42.96	1.606	0.0706
	ZR soil-1	M2	0.013	−806.8	0.988		103.64	10.56	2.603	0.045
	ZR soil-2	M2	0.0166	−767.6	0.979		13.07	1.33	4.62	0.983
	Sand	M3	0.022	−459	0.972	0.765	0.416	0.099		
	TR soil-1	M3	0.104	−338.5	0.949	0.765	128.81	567.92		
	TR soil-2	M3	0.102	−341.9	0.818	0.765	200.33	182.71		
	ZR soil-1	M3	0.0809	−471.7	0.897	0.765	368.88	319		
	ZR soil-2	M3	0.0845	−463.5	0.868	0.765	296.38	245.36		
	Sand	M4	0.22	−456.6	0.972	0.765	0.440	0.287	3.21	37.03
	TR soil-1	M4	0.055	−430.4	0.968	0.765	1118.8	514.97	2.09	0.284
	TR soil-2	M4	0.042	−471.2	0.968	0.765	7517	225.45	1.60	0.05
	ZR soil-1	M4	0.0206	−726.7	0.962	0.765	1400.1	115	8.03	0.858
	ZR soil-2	M4	0.0165	−763.4	0.980	0.765	2874.6	257.7	2.33	0.06

Different models were used in simulations: attachment and detachment (M1); attachment, detachment, and blocking (M2); depth-dependent retention (M3); and blocking combined with depth-dependent retention (M4). k_{att} - first-order attachment rate, β - empirical parameter, S_{max} - the maximum solid phase concentration of deposited AgNPs, AIC - Akaike Information Criterion, RMSE - root mean square errors, and SE - standard error.

fits for the NP transport in the soil and sand columns using a similar model (Cornelis et al., 2013; Liang et al., 2013a,b; Braun et al., 2015). Low attachment on the sand surfaces, as quantified by a small value of k_{att}, explains the high effluent concentrations. Liang et al. (2013a) reported that when k_{att} is too small, the breakthrough occurs with no retardation and the effluent concentrations slowly increase with time as the favorable retention locations are gradually filled. Overall, the blocking effects were not observed to play a significant role in the quartz sand columns.

Lower values of k_{att} for the sand columns compared to the soil columns may be attributed to the effect of a collector particle size on the AgNPs transport and retention (Table 5). However, the same trend was not observed between the two soil columns. The k_{att} values for the TR soil with a higher median grain size (see Table 1) were larger than the corresponding values for the ZR soil. However, S_{max}/C_o values for the ZR soil were higher than the corresponding values for the TR soil (Table 5).

Detachment is mostly interpreted by the deposition of AgNPs in the secondary minimum and their subsequent removal due to changes in hydrochemical conditions (Braun et al., 2015). In our study, experimental data was described only as an attachment process, while assuming that detachment was negligible. A detachment of nanoparticles during deposition experiments is almost always negligible (Liang et al., 2013a,b). There is nearly no secondary energy minimum in their interactions with surfaces because of their small size (Petosa et al., 2010). Moreover, detachment would manifest itself in the BTC as tailing, which was not very pronounced in soil columns. Kumahor et al. (2015) suggested that the huge difference between k_{att} and k_{det} indicates fast attachment to the SWI and slow detachment.

The model simulations confirm that a Langmuir blocking model (Eq. (4)) is sufficient to closely fit the behavior of RPs in the soil columns. Overall, it may be concluded that attachment of AgNPs is irreversible in many cases. This finding is consistent with the experimental results, in which high retention and very little recovery (< 1%) of AgNPs in the effluent were observed under both flow conditions (see Fig. 3b,c and Table 4).

Retarded BTCs can be described using fitted parameters k_{att} and S_{max}/C_o in Eqs. (3) and (4), which are related to the retention rate and the AgNPs sorption capacity, respectively (Liang et al., 2013a). Liang et al. (2013a) suggested that a high value of k_{att} produces a complete NP retention until S_{max}/C_o is filled. Consequently, when the values of k_{att} and S_{max}/C_o are large, more retarded BTCs are expected (Liang et al., 2013a). Hence, the stronger AgNP retention in the ZR soil compared with the TR soil can be explained by an increase in the fitted values of

S_{max}/C_o in the ZR soil (Table 5), which occurs due to the enhancement of the effects of nanoscale heterogeneities and a decreased grain size, which is in agreement with Liang et al. (2013a,b) and Sagee et al. (2012). On the other hand, greater k_{att} for the TR soil when compared with the ZR soil may be attributed to the other soil physical properties such as soil structure and dead-end and/or non-continuous pores, which were probably formed in the weakly-structured TR soil (see the MWD values in Table 1).

4. Conclusions

1) Results of this study have several implications for the understanding of the transport and retention of AgNPs in the saturated and unsaturated sand and soils. Quartz sand surfaces are unfavorable for the AgNP deposition and result in a high mobility of AgNPs through the sand columns. Moreover, the limited transport of PVP-stabilized AgNPs in the undisturbed soil experiments suggests that AgNPs rapidly interact with the natural soils. The high retention of AgNPs in soil may be a result of favorable deposition of AgNPs on soil colloids and/or straining of AgNPs enhanced by the formation of heteroaggregates.
2) The effects of soil texture and a degree of water saturation on the transport and retention of AgNPs in soil have been investigated. These variables, by affecting the hydrodynamic factors, distribution and continuity of pores, deposition, filtration and sorption, complicate the description of the AgNPs transport in the soil. The ZR soil with higher surface area filters AgNPs more than the TR soil does. Despite its lower surface area and smaller Freundlich coefficient, the retention of AgNPs in the TR soil is not significantly different from the more structured ZR soil. In addition, the presence of air under unsaturated conditions has only a small effect on the retention and transport of AgNPs in most experiments.
3) The one-site kinetic attachment model provides a good description of the retention profiles (RPs) of AgNPs under both saturated and unsaturated flow conditions. However, the model fitting parameters could not be successfully used to explain the BTCs of AgNPs under various saturation conditions in the natural soil columns, partly due to very small values of effluent concentrations. The results demonstrate that AgNPs transport studies in natural soils need to consider retarded BTCs, hyperexponential RPs, and colloid associations, which are factors commonly neglected in repacked sand column experiments.
4) The high retention and limited mobility of AgNPs in natural calcareous soil systems under saturated or unsaturated conditions observed in this study suggest that there is only a low risk of off-site transport vertically into the subsurface or laterally into nearby sites. However, further research is needed to understand reactions and transformations which may re-mobilize AgNPs in the soils. A more robust model is also required to consider the transport and deposition behavior of AgNPs.

Acknowledgments

We expressed our appreciation to the Isfahan University of Technology for the financial support of the research.

References

Akaike, H., 1998. A new look at the statistical model identification. In: Parzen, E., Tanabe, K., Kitagawa, G. (Eds.), Selected Papers of Hirotugu Akaike. Springer, New York, pp. 215–222.
Blake, G.R., Hartge, K.H., 1986. Bulk density. In: Klute, A. (Ed.), Methods of Soil Analysis: Part 1, Physical and Mineralogical Methods, Second ed. ASA/SSSA, Monograph 9, Madison, WIpp. 374–380.
Bradford, S.A., Torkzaban, S., 2008. Colloid transport and retention in unsaturated porous media: a review of interface-, collector-, and pore-scale processes and models. Vadose Zone J. 7 (2), 667–681.
Bradford, S.A., Yates, S.R., Bettahar, M., Šimůnek, J., 2002. Physical factors affecting the transport and fate of colloids in saturated porous media. Water Resour. Res. 38 (12), 1327. http://dx.doi.org/10.1029/2002WR001340.
Bradford, S.A., Šimůnek, J., Bettahar, M., van Genuchten, M.Th., Yates, S.R., 2003. Modeling colloid attachment, straining, and exclusion in saturated porous media. Environ. Sci. Technol. 37 (10), 2242–2250.
Bradford, S.A., Bettahar, M., Šimůnek, J., van Genuchten, M.Th., 2004. Straining and attachment of colloids in physically heterogeneous porous media. Vadose Zone J. 3 (2), 384–394.
Bradford, S.A., Šimůnek, J., Bettahar, M., van Genuchten, M.Th., Yates, S.R., 2006. Significance of straining in colloid deposition: evidence and implications. Water Resour. Res. 42 (12), W12S15. http://dx.doi.org/10.1029/2005WR004791.
Bradford, S.A., Torkzaban, S., Leij, F.J., Šimůnek, J., 2015. Equilibrium and kinetic models for colloid release under transient solution chemistry conditions. J. Contam. Hydrol. 181, 141–152.
Braun, A., Klumpp, E., Azzam, R., Neukum, C., 2015. Transport and deposition of stabilized engineered silver nanoparticles in water saturated loamy sand and silty loam. Sci. Total Environ. 535, 102–112. http://dx.doi.org/10.1016/j.scitotenv.2014.12.023.
Carbone, S., Vittori Antisari, L., Gaggia, F., Baffoni, L., Di Gioia, D., Vianello, G., Nannipieri, P., 2014. Bioavailability and biological effect of engineered silver nanoparticles in a forest soil. J. Hazard. Mater. 280, 89–96. http://dx.doi.org/10.1016/j.jhazmat.2014.07.055.
Chen, G., Flury, M., 2005. Retention of mineral colloids in unsaturated porous media as related to their surface properties. Colloids Surf. A Physicochem. Eng. Asp. 256 (2–3), 207–216.
Chen, L., Sabatini, D.A., Kibbey, T.C.G., 2008. Role of the air–water interface in the retention of TiO_2 nanoparticles in porous media during primary drainage. Environ. Sci. Technol. 42 (6), 1916–1921.
Cornelis, G., Kirby, J.K., Beak, D., Chittleborough, D., McLaughlin, M.J., 2010. A method for determination of retention of silver and cerium oxide manufactured nanoparticles in soils. Environ. Chem. 7 (3), 298–308.
Cornelis, G., Casey, D., McLaughlin, M.J., Kirby, J.K., Beak, D.G., Chittleborough, D., 2012. Retention and dissolution of engineered silver nanoparticles in natural soils. Soil Sci. Soc. Am. J. 76 (3), 891–902. http://dx.doi.org/10.2136/sssaj2011.0360.
Cornelis, G., Pang, L., Doolette, C., Kirby, J.K., McLaughlin, M.J., 2013. Transport of silver nanoparticles in saturated columns of natural soils. Sci. Total Environ. 463–464, 120–130. http://dx.doi.org/10.1016/j.scitotenv.2013.05.089.
Dousset, S., Thevenot, M., Pot, V., Šimunek, J., Andreux, F., 2007. Evaluating equilibrium and non-equilibrium transport of bromide and isoproturon in disturbed and undisturbed soil columns. J. Contam. Hydrol. 94 (3–4), 261–276.
El Badawy, A.M., Luxton, T.P., Silva, R.G., Scheckel, K.G., Suidan, M.T., Tolaymat, T.M., 2010. Impact of environmental conditions (pH, ionic strength, and electrolyte type) on the surface charge and aggregation of silver nanoparticles suspensions. Environ. Sci. Technol. 44, 1260–1266.
El Badawy, A.M., Hassan, A.A., Scheckel, K.G., Suidan, M.T., Tolaymat, T.M., 2013. Key factors controlling the transport of silver nanoparticles in porous media. Environ. Sci. Technol. 47 (9), 4039–4045.
Espinasse, B., Hotze, E.M., Wiesner, M.R., 2007. Transport and retention of colloidal aggregates of C_{60} in porous media: effects of organic macromolecules, ionic composition, and preparation method. Environ. Sci. Technol. 41 (21), 7396–7402.
Fang, J., Xu, M.-J., Wang, D.-J., Wen, B., Han, J.-Y., 2013. Modeling the transport of TiO_2 nanoparticle aggregates in saturated and unsaturated granular media: effects of ionic strength and pH. Water Res. 47 (3), 1399–1408.
Gee, G.W., Bauder, J.W., 1986. Particle-size analysis. In: Klute, A. (Ed.), Methods of Soil Analysis: Part 1, Physical and Mineralogical Methods. Agronomypp. 383–411.
He, D., Jones, A.M., Garg, S., Pham, A.N., Waite, T.D., 2011. Silver nanoparticle–reactive oxygen species interactions: application of a charging–discharging model. J. Phys. Chem. C 115 (13), 5461–5468.
Hotze, E.M., Phenrat, T., Lowry, G.V., 2010. Nanoparticle aggregation: challenges to understanding transport and reactivity in the environment. J. Environ. Qual. 39 (6), 1909–1924.
Ito, T., Sun, L., Bevan, M.A., Crooks, R.M., 2004. Comparison of nanoparticle size and electrophoretic mobility measurements using a carbon-nanotube-based coulter counter, dynamic light scattering, transmission electron microscopy, and phase analysis light scattering. Langmuir 20 (16), 6940–6945.
Kasel, D., Bradford, S.A., Šimůnek, J., Heggen, M., Vereecken, H., Klumpp, E., 2013a. Transport and retention of multi-walled carbon nanotubes in saturated porous media: effects of input concentration and grain size. Water Res. 47 (2), 933–944.
Kasel, D., Bradford, S.A., Šimůnek, J., Pütz, T., Vereecken, H., Klumpp, E., 2013b. Limited transport of functionalized multi-walled carbon nanotubes in two natural soils. Environ. Pollut. 180, 152–158.
Klute, A., Dirksen, C., 1986. Hydraulic conductivity and diffusivity: laboratory methods. In: Klute, A. (Ed.), Methods of Soil Analysis: Part 1, Physical and Mineralogical Methods, second ed. ASA/SSSA, Monograph 9, Madison, WIpp. 678–732.
Kumahor, S.K., Hron, P., Metreveli, G., Schaumann, G.E., Vogel, H.-J., 2015. Transport of citrate-coated silver nanoparticles in unsaturated sand. Sci. Total Environ. 535, 113–121.
Liang, Y., Bradford, S.A., Šimůnek, J., Heggen, M., Vereecken, H., Klumpp, E., 2013a. Retention and remobilization of stabilized silver nanoparticles in an undisturbed loamy sand soil. Environ. Sci. Technol. 47 (21), 12229–12237.
Liang, Y., Bradford, S.A., Šimůnek, J., Vereecken, H., Klumpp, E., 2013b. Sensitivity of the transport and retention of stabilized silver nanoparticles to physicochemical factors. Water Res. 47 (7), 2572–2582.
Lin, S., Cheng, Y., Bobcombe, Y., Jones, K.L., Liu, J., Wiesner, M.R., 2011. Deposition of silver nanoparticles in geochemically heterogeneous porous media: predicting affinity from surface composition analysis. Environ. Sci. Technol. 45 (12), 5209–5215.

Lin, S., Cheng, Y., Liu, J., Wiesner, M.R., 2012. Polymeric coatings on silver nanoparticles hinder autoaggregation but enhance attachment to uncoated surfaces. Langmuir 28 (9), 4178–4186.
Loeppert, R.H., Suarez, D.L., 1996. Carbonate and gypsum. In: Sparks, D.L., Page, A.L., Helmke, P.A., Loeppert, P.N., Soltanpour, P.N., Tabatabai, M.A., Johnson, C.T., Sumner, M.E. (Eds.), Method of Soil Analysis. Part 2: Chemical Properties. Soil Science Society of America, Inc. American Society of Agronomy, Madison, Wisconsin, USA, pp. 437–474.
Majeed Khan, M.A., Kumar, S., Ahamed, M., Alrokayan, S.A., AlSalhi, M.S., 2011. Structural and thermal studies of silver nanoparticles and electrical transport study of their thin films. Nanoscale Res. Lett. 6 (1), 434.
Matthess, G., Pekdeger, A., Schroeter, J., 1988. Persistence and transport of bacteria and viruses in groundwater – a conceptual evaluation. J. Contam. Hydrol. 2 (2), 171–188.
McCarthy, J.F., McKay, L.D., 2004. Colloid transport in the subsurface: past, present, and future challenges. Vadose Zone J. 3 (2), 326–337. http://dx.doi.org/10.2113/3.2.326.
Moore, D.M., Reynolds, R.C., 1997. X-ray Diffraction and the Identification and Analysis of Clay Minerals. Oxford University Press, Oxford New York.
Nelson, D.W., Sommers, L.E., 1996. Total carbon, organic carbon, and organic matter. In: Sparks, D.L., Page, A.L., Helmke, P.A., Loeppert, P.N., Soltanpour, P.N., Tabatabai, M.A., Johnson, C.T., Sumner, M.E. (Eds.), Method of Soil Analysis. Part 2: Chemical Properties. Soil Science Society of America, Inc. American Society of Agronomy, Madison, Wisconsin, USA, pp. 961–1010.
Neukum, C., Braun, A., Azzam, R., 2014. Transport of stabilized engineered silver (Ag) nanoparticles through porous sandstones. J. Contam. Hydrol. 158, 1–13. http://dx.doi.org/10.1016/j.jconhyd.2013.12.002.
Nowack, B., Bucheli, T.D., 2007. Occurrence, behavior and effects of nanoparticles in the environment. Environ. Pollut. 150 (1), 5–22.
Pachapur, V.L., Dalila Larios, A., Cledón, M., Brar, S.K., Verma, M., Surampalli, R.Y., 2016. Behavior and characterization of titanium dioxide and silver nanoparticles in soils. Sci. Total Environ. 563–564, 933–943. http://dx.doi.org/10.1016/j.scitotenv.2015.11.090.
Peralta-Videa, J.R., Zhao, L., Lopez-Moreno, M.L., de la Rosa, G., Hong, J., Gardea-Torresdey, J.L., 2011. Nanomaterials and the environment: a review for the biennium 2008–2010. J. Hazard. Mater. 186 (1), 1–15.
Petosa, A.R., Jaisi, D.P., Quevedo, I.R., Elimelech, M., Tufenkji, N., 2010. Aggregation and deposition of engineered nanomaterials in aquatic environments: role of physicochemical interactions. Environ. Sci. Technol. 44 (17), 6532–6549.
Rahmatpour, S., Shirvani, M., Mosaddeghi, M.R., Nourbakhsh, F., Bazarganipour, M., 2017. Dose–response effects of silver nanoparticles and silver nitrate on microbial and enzyme activities in calcareous soils. Geoderma 285 (1), 313–322.
Safadoust, A., Mahboubi, A.A., Gharabaghi, B., Mosaddeghi, M.R., Voroney, P., Unc, A., Sayyad, G., 2011. Bacterial filtration rates in repacked and weathered soil columns. Geoderma 167–168, 204–213.
Sagee, O., Dror, I., Berkowitz, B., 2012. Transport of silver nanoparticles (AgNPs) in soil. Chemosphere 88 (5), 670–675.
Seyfried, M.S., Rao, P.S.C., 1987. Solute transport in undisturbed columns of an aggregated tropical soil: preferential flow effects. Soil Sci. Soc. Am. J. 51, 1434–1444.
Šimůnek, J., Šejna, M., Saito, H., Sakai, M., van Genuchten, M.Th., 2008. The HYDRUS-1D software package for simulating the movement of water, heat, and multiple solutes in variably saturated media. In: HYDRUS Software Series 3. Department of Environmental Sciences, University of California Riverside, Riverside, California, USA, pp. 315. Version 4.0.
Šimůnek, J., van Genuchten, M.Th., Šejna, M., 2016. Recent developments and applications of the HYDRUS computer software packages. Vadose Zone J. 15 (7), 25. http://dx.doi.org/10.2136/vzj2016.04.0033.
Sumner, M.E., Miller, W.P., 1996. Cation exchange capacity, and exchange coefficients. In: Sparks, D.L., Page, A.L., Helmke, P.A., Loeppert, P.N., Soltanpour, P.N., Tabatabai, M.A., Johnson, C.T., Sumner, M.E. (Eds.), Methods of Soil Analysis. Part 2: Chemical Properties, 3rd ed. ASA, SSSA, CSSA, Madison, WI, pp. 1201–1229.
Torkzaban, S., Bradford, S.A., van Genuchten, M.Th., Walker, S.L., 2008. Colloid transport in unsaturated porous media: the role of water content and ionic strength on particle straining. J. Contam. Hydrol. 96 (1), 113–127.
Torkzaban, S., Kim, Y., Mulvihill, M., Wan, J., Tokunaga, T.K., 2010. Transport and deposition of functionalized CdTe nanoparticles in saturated porous media. J. Contam. Hydrol. 118 (3), 208–217.
Tufenkji, N., Elimelech, M., 2004. Correlation equation for predicting single-collector efficiency in physicochemical filtration in saturated porous media. Environ. Sci. Technol. 38 (2), 529–536.
Yoder, R.E., 1936. A direct method of aggregate analysis and study of physical nature of erosion losses. J. Am. Soc. Agron. 28 (5), 337–351.
Zhang, M., Bradford, S.A., Šimůnek, J., Vereecken, H., Klumpp, E., 2017. Roles of cation valance and exchange on the retention and colloid-facilitated transport of functionalized multi-walled carbon nanotubes in a natural soil. Water Res. 109, 358–366. http://dx.doi.org/10.1016/j.watres.2016.11.062. (2017).
Zhu, Y.-P., Wang, X.-K., Guo, W.-L., Wanga, J.-G., Wang, C., 2010. Sonochemical synthesis of silver nanorods by reduction of sliver nitrate in aqueous solution. Ultrason. Sonochem. 17 (4), 675–679.